A theoretical study of As4S4: Bonding, vibrational analysis and infrared and Raman spectra

ARTICLE *in* JOURNAL OF MOLECULAR STRUCTURE THEOCHEM · MAY 2003

Impact Factor: 1.37 · DOI: 10.1016/S0166-1280(02)00746-7

3 AUTHORS, INCLUDING:

Ajit Banerjee
University of Utah
54 PUBLICATIONS **1,187** CITATIONS

ELSEVIER

Journal of Molecular Structure (Theochem) 626 (2003) 63–75

THEO CHEM

www.elsevier.com/locate/theochem

A theoretical study of As_4S_4: Bonding, vibrational analysis and infrared and raman spectra

Ajit Banerjee[a,b,*], James O. Jensen[a], Janet L. Jensen[b]

[a]*Edgewood Research, Development, and Engineering Center, Aberdeen Proving Ground, MD 21010-5423, USA*
[b]*Science Applications International Corporation, Aberdeen Proving Ground, MD 21010-5423, USA*

Received 20 September 2002; accepted 15 October 2002

Abstract

The structure, bonding, electron distribution, normal mode frequencies and the corresponding vibrational assignments of tetrarsenic tetrasulfide (As_4S_4) in D_{2d} symmetry are examined theoretically using the GAUSSIAN 98 set of quantum chemistry codes at the HF, MP2 and B3LYP(DFT) levels of theory using the standard 6-311G* basis. By comparison to experimental normal mode frequencies deduced by Chapman [Spectrochim. Acta 24A(1968)1687] correction factors for predominant vibrational motions are determined and compared. Normal modes were decomposed into four nonredundant motions {As– As stretch, As– S stretch, As–S–As bend, and As–S–As wagging modes}.

Keywords: Vibrations; Normal mode frequencies; Infrared spectra; Raman spectra; Tetrarsenic tetrasulfide

1. Introduction

Arsenic Chalogenides As_4S_4, As_4Se_4, and As_4S_6, are very interesting class of compounds from scientific as well as from practical usage. For similar range of temperature and pressure, these substances are both crystalline as well as amorphous and have similar properties in either form. Because of their photochemical sensitivity Arsenic Chalogenides are important for their use in optics [1]. They have been used as photoresists in optical and ultraviolet lithography, optical memory devices, switches, modulators and optical computing and use as a p–n junctions [2].

The Tetraarsenic tetrasulfide, As_4S_4, exists in four different crystalline modifications. The Realgar (α-As_4S_4) is the low temperature polymorpf and a molecular mineral. The β-As_4S_4 is obtained by heating the α-As_4S_4 above 260 °C or heating a mixture of As and S in stoichiometric proportions. In both forms, As_4S_4 has a cage-like structure and bonding is predominantly covalent. They belong to the same molecular symmetry however different packing in solid state. Kutoglu [3] synthesized another As_4S_4 polymorph with different molecular structure by re-crystallizing a quenched AsS melt from 500–600 °C to the room temperature. The fourth, and the most recent form called

* Corresponding author. Address: Edgewood Research, Science Applications International Corporation, Development and Engineering Center, Aberdeen Proving Ground, MD 21010-5423, USA.
E-mail address: ajit.banerjee@sbccom.apgea.army.mil (A. Banerjee).

0166-1280/03/$ - see front matter © 2002 Elsevier Science B.V. All rights reserved.
PII: S0166-1280(02)00746-7

the pararealgar was first identified by Roberts et al. [4]. It has molecular structure identical to Kutoglu [3,5]. Besides these polymorphs with more studied crystal structures, another phase, called χ-phase was found [6], which has very similar structure as the β-phase.

There have been several other experimental and theoretical studies through the years of varying importance. In seventies, many types of measurements optical, crystallographic, X-ray diffraction [7,8] and semi-empirical theoretical have been reported, there seemed to be little consentious about the relative arrangement of the atoms in gas amorphous and solid phases. Babić and Rabii [9,10] have performed local-density pseudopotential calculations. They have found that the As–As bond is the main reason for the stability of arsenic sulfides and excellent transferability of the As–S bond charge density among the molecules have been found. Yamabe et al. [11]have studied As_4S_5 molecule by semi-empirical intermediate neglect of differential overlap method. The analysis of binding energy from molecule to molecule suggests a reason for the relative abundance of As_4S_4 in arsenic sulfide gas phase. It is the stability of the As–As bond. As_4S_4 is most likely closed packed. Adding each extra sulfur atoms As_4S_5, As_4S_6, etc. breaks an As–As bond and pushes the As atoms apart. The experimental As–S bond distance is in the range of 2.23–2. 35 Å[12,13].

In this paper, we shall perform calculations, on the α realgar form of As_4S_4, using three different ab initio quantum chemical methods to obtain information on structure, the normal mode frequencies, the corresponding vibrational assignments, and the elctronic properties. The methods are the Hartree–Fock (HF), the Second-order Moller–Plesset (MP2*), and the Density Functional(DFT/B3LYP) using the GAUSSIAN 98 set of quantum chemistry codes with the standard 6-311G* basis. The reason for using these three well-established methods to make sure that our results do not suffer from idiosyncrasies of any of one particular method. Some results, which show marked departure from the existing data, can be crosschecked against the results obtained from the other two methods. The HF method should give us broad qualitative overview and the DFT and MP2 provide more refined data. The realgar α-As_4S_4 is examined in D_{2d} symmetry. By comparison to experimental normal mode frequencies deduced by Chapman [28] correction factors for predominant vibrational motions are determined and compared. Normal modes were decomposed into four non-redundant motions {As–As stretch, As–S stretch, As–S–As bend, and As–S–As wagging modes}.

2. Bonding and vibrational modes

2.1. Structure and electron distribution

The structure and the vibrational frequencies of As_4S_4 at the Hartree–Fock (HF) [14], second-order Moller–Plesset (MP2) [15], and Density Functional Theory (DFT) [16] using the exchange correlation function B3LYP [17,18] levels of theory are calculated using the standard 6-31G* basis set. The calculations were first performed using the GAUSSIAN 94 Program Package [19] running on a four processor SGI O200 computer or an SGI Origin 2000 computer at the Army Research Laboratory High Performance Computing Center.

To understand the bonding in this molecule we analyzed the electron distributions and the nature of the occupied valence orbitals, which can have symmetry a_1, a_2, e, t_1, or t_2 The electronic distribution can be studied in terms of the 1-electron density matrix

$$P_{\mu\nu} = 2\sum_{i=1}^{occ} c_{\mu i}c_{\nu i} \tag{1}$$

where $c_{\mu i}$ is molecular orbital coefficient for atomic orbital μ in the ith molecular orbital and $c_{\nu i}$ is molecular orbital coefficient for atomic orbital ν in the ith molecular orbital. From the 1-electron density matrix, the total overlap population (also known as the Mulliken electron population) between two atomic centers A and B, Q_{AB}, can be determined from

$$Q_{AB} = 2\sum_{\mu}^{A}\sum_{\nu}^{B} P_{\mu\nu}S_{\mu\nu} \tag{2}$$

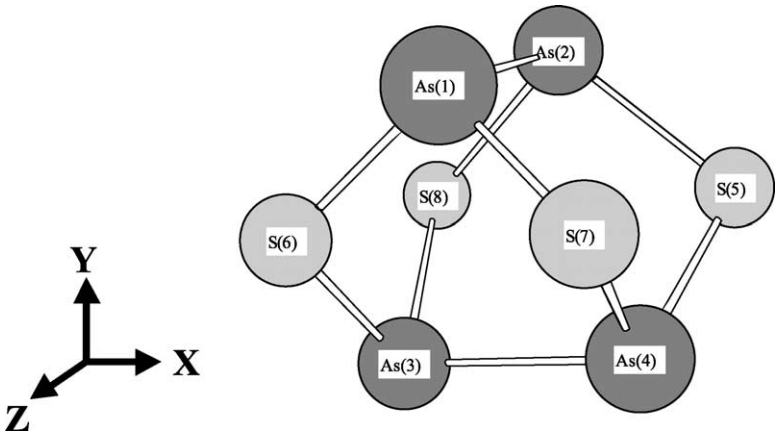

Fig. 1. Structure of As_4S_4.

where the summation over μ and ν goes over all basis functions on atoms A and B, respectively, and $S_{\mu\nu}$ is the overlap matrix element between atomic orbital μ and atomic orbital ν. The total overlap populations provide quantitative information about the bonding between atoms. A large positive value indicates a significant electron population in the region between A and B, which has been shifted from the immediate vicinity of the individual atoms. This is a typical characteristic of strong A–B bonding. On the other hand, a negative value of Q_{AB} implies that the electrons have been displaced away from the interatomic region, characteristic of an A–B interaction which is antibonding.

As seen in Fig. 1, the equilibrium geometry for the α-form of As_4S_4 has a cage like molecular structure with D_{2d} symmetry. The results show that each arsenic atom is bonded directly to another arsenic atom and with two sulfur atoms. Furthermore, one arsenic atom and has two sulfur and two arsenic atoms as second neighbors. The As atoms labeled 1and 2 reside in the yz-plane parallel to the *y*-axis and equidistant from the *z*-axis. Similarly As atoms 3 and 4 reside in the perpendicular xy-plane equidistant from the *z*-axis. Thus the atoms 1, 2 and 3,4 are symmetry equivalent. Similarly all near neighbor S atoms are also symmetry equivalent via the operation C_2. The HF calculation results show that the neighboring symmetry equivalent As atoms have a bond length of 2.55 Å = *d*(As–As) and the corresponding S atoms bonds are *d*(As–S) = 2.24 Å. Fig. 1 and Table 1 show the structure. The neighboring As–As bonds (viz. 1-2 and 3-4) are the most dominant bonds with $Q_{As-As} = 0.298$ compared to the neighboring As–S(e.g. 6-1-7, 5-2-8, 6-3-8, and 5-4-7) bonds with $Q_{As-S} = 0.237$, and weakly bonded diagonal S atoms(5-6 and 7-8) with $Q_{S-S} = 0.002$.

Table 1
Calculated geometries for ground electronic state of As_4S_4 in D_{2d} symmetry at three levels of calculation; for comparison the average experimental geometrical coordinates[a] in crystalline As_4S_4 are also listed

Geometrical coordinate	HF/6-311G*	MP2/6-311G*	B3LYP/6-311G*	Exp. ave [27]
R(As–	256	260	264	256
R(S–As)/pm	224	224	227	224
∠As–S–As/°	100.3	100.8	101.2	
∠S–As–S/°	95.1	95.6	95.5	92,94,101[a]
∠As–As–S/°	99.6	99.2	99.1	

[a] Alpha, beta, and pararealgar forms (large spread) [27].

All other bonds show either barely bonding character or are non-bonding with negative Q values, among these are the bonding between the non-neighboring As atoms with Q values of -0.086 and neighboring S atoms with -0.076. Overall, the electron distribution has shifted somewhat toward each of the equivalent S atoms rendering them electronegative with population density of 0.34 and thus each of the As atoms are now electropositive by the same amount. The other calculations, we have performed, MP2, and DFT, also confirm these results differing slightly in numerical values.

Next, we describe the bonding characteristics and electron distributions of all 23 occupied valence molecular orbitals 77–98. This set includes the highest occupied electrons from each of the four S- and As atoms; six 3p electrons of S and five 4p electrons of the As atom. They span the range of orbital energies from -1.07 to -0.33 au. The molecular valence orbital 77 is totally symmetric of A_1 type with orbital energy of -1.07 au. It consists of four S–As–S, σ-bonds between s-orbitals of the respective S and As atoms, $(S)_s^6 + (As)_s^1 + (S)_s^7$ and between other similar trio of atoms numbered 5-2-8; 6-3-8 and 5-4-7. The Fig. 2 clearly shows this bonding in a pictorial form. The convention we have used is that, e.g. $(As)_s^2 + (S)_s^8$ refers to a sum of the atomic orbital s of the As atom 2 to that of sulfur atom 6. We also refer to the atoms by their respective numbering shown in Fig. 1 when the text does not require specific orbital or sign(+ or −) association. The mos 78 and 79 are of *E*-symmetry shown in Fig. 2 has a look of two π-lobes, which are however are two sets of σ-orbitals of opposite signs. Specifically, mo 78 consists of σ-bonding from valence s- atomic orbital contributions from S and As atoms, $(S)_s^6 + (As)_s^1 + (S)_s^7$ and $-\{(S)_s^5 + (As)_s^2 + (S)_s^8\}$, but of opposite signs and σ-antibonding $(S)_s^5 - (S)_s^7$ and $(S)_s^6 - (S)_s^8$. The mo 79, the e-twin shows the S–As–S σ-bonding involving atoms 6-3-8 and 5-4-7, and σ-antibonding involving atoms 6-7 and 5-8. The mo 80 of B_1 symmetry consists of only s orbitals contributions from adjacent S atoms; $(S)_s^6 - (S)_s^8$ and $(S)_s^5 - (S)_s^7$ giving it an antibonding character. The mo 81 is of B_2 symmetry and of orbital energy -0.87 au. It consists of s orbitals of the near neighbor As atoms to give σ-bonds, except with opposite signs; $\{(As)_s^1 + (As)_s^2\}$ and $-\{(As)_s^2 + (As)_s^4\}$. Thus, it has a look a π-lobe encompassing the entire molecule. The mo 82 is a totally symmetric A_1 type with orbital energy of -0.74. It again consists of a near neighbor bonding with s-orbitals of As atoms 1-2 and 3-4. In addition, it also has an antibonding component between al diagonal As and S atoms, e.g. $(As)_s^1 - (S)_s^8$. Orbitals 83 and 84 are degenerate E-type orbital of energy -0.71 au. It consists of largely σ-antibonding s combinations between all near neighbor As atoms; $(As)_s^1 - (S)_s^2$, and similarly $(As)_s^3 - (S)_s^4$. So far, all the valence molecular orbitals have involved only the s-type valence atomic orbitals of the respective atoms As and S. Starting orbitals 83, we see involvement of p and d orbitals from the participating atoms. Orbital 85 is B_2 type consisting of σ-bonding between s as well as the d-orbitals $\{(As)^1_{s,dxx,\ dyy,\ dzz} + (As)^2_{s,dxx,\ dyy,\ dzz}\}$, and similarly for 3-4 but of opposite sign giving a virtual π-character. In addition, it has components of σ-bonds of all S–As–S type, e.g. $(S)^6_{s+py\ -\ pz} + (As)_{s+px\ +\ py}{}^1 + (S)^7_{s+py\ -\ pz}$ showing $s + p_x + p_y$ hybridization. Orbital 86 is of A_2 symmetry of energy -0.52 au. It has several distinct components; an antibonding π-component, $\{(As)^1_{px} - (As)^2_{px}\}$, and $-\{(As)^1_{py} - (As)^2_{py}\}$; bonding π-component between diogonal S atoms $\{(S)^5_{pz} + (S)^6_{pz}\}$- and $\{(S)^7_{pz} + (S)^8_{pz}\}$; and an antibonding π-component between the neighboring S atoms $\{(S)^5_{pz} - (S)^7_{pz}\}$,$\{(S)^6_{pz} - (S)^8_{pz}\}$. Orbital 87 is totally symmetric of energy -0.51 au. This again shows σ-bonding between diagonal S atoms 5-6, and 7-8, e.g. $\{(S)^5_{px,py} - (S)^6_{px,py}\}$and $\{(S)^5_s + (S)^6_s\}$. Orbital 88 and 89 are *e-twins of energy −0.49 au. and with several components. It involves π-bonding between the As 1-2; $\{(As)^1_{px} + (As)^2_{px}\}$ and several bonding and antibonding σ-and π-components involving As−-S; 3-6, 3-8, 4-5, and 4-7, as well as S–S between near neighbors; 5-7, 6-8. The twin orbital 89 has the role of As 1,and 2 changed to As 3,and 4, respectively Orbitals 90, 91 are again e-twins of energy −0.42 au. And these are qualitatively similar to the orbital 88, 89 twins.*

The molecular orbital 92 is of B_1 symmetry consists of π-bonds between neighboring As atoms; superposition of p_x orbitals on centers 1 and 2 and p_y orbitals on centers 3 and 4. In addition it

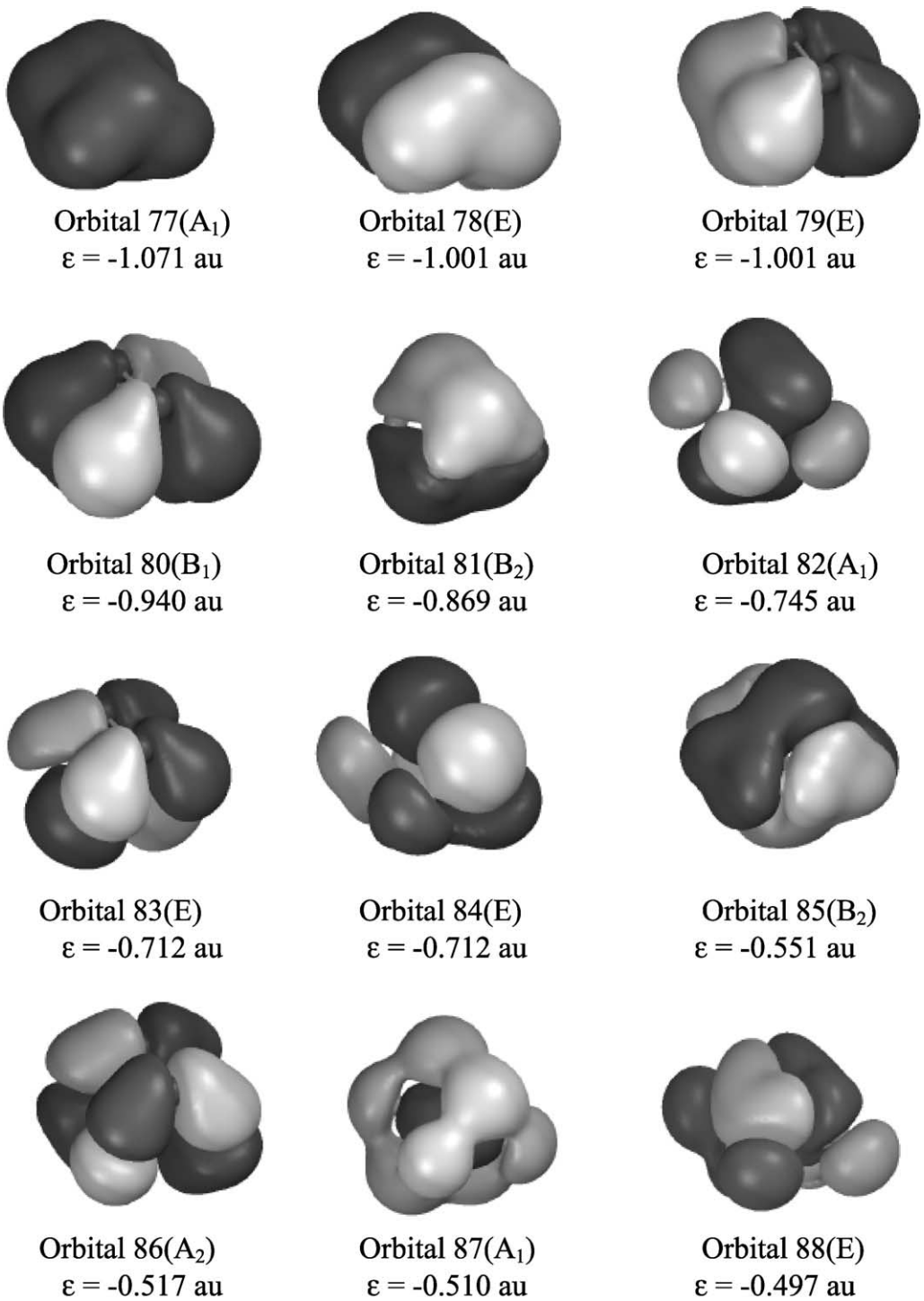

Fig. 2. Selected molecular orbitals of As_4S_4.

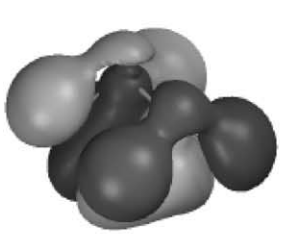

Orbital 89(E)
ε = -0.497 au

Orbital 90(E)
ε = -0.425 au

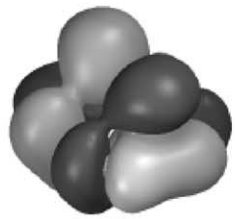

Orbital 91(E)
ε = -0.425 au

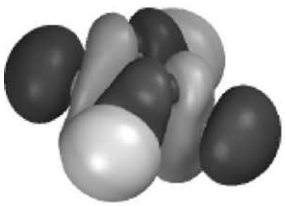

Orbital 92(B_1)
ε = -0.416 au

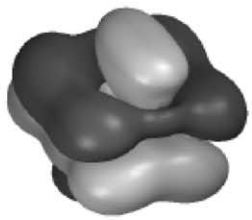

Orbital 93(B_2)
ε = -0.401 au

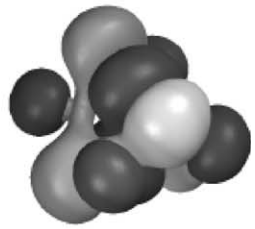

Orbital 94(A_1)
ε = -0.388 au

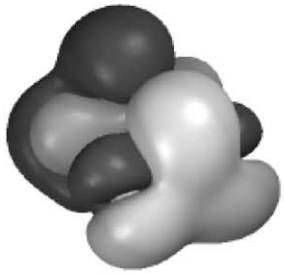

Orbital 95(E)
ε = -0.386 au

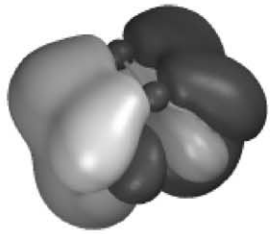

Orbital 96(E)
ε = -0.386 au

Orbital 97(A_2)
ε = -0.360 au

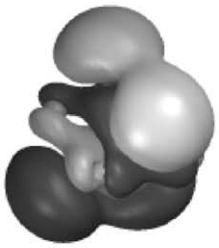

Orbital 98(B_2)
ε = -0.338 au

Fig. 2 (*continued*)

consists of antibonding character generated by a combination p_x and p_y ao on each of the S atoms, e.g. $\{(S)^5_{px} + (S)^8_{px}\}$ and $\{(S)^5_{py} + (S)^7_{py}\}$ The molecular orbital 93 is of B_2 symmetry and consists of σ-bonds between neighboring As–As symmetry equivalent atoms, i.e. between 1-2 and 3-4, and π-bonds between neighboring S atoms; 5-6-7-8. The σ-bonds are superposition of s-type atomic orbitals (ao) centered on each As atoms. While the π-bonds are superposition of the p_z-type ao on S each atoms resulting a ring of positive and negative electron densities above and below the plane of S atoms. The molecular orbital 94 is the highest occupied mo of the A_1 symmetry. It consists of As–As σ-bonds, between atoms 1-2 and between 3-4, constructed from superpositions of s- and p_y-type ao centered on each As atom. The other bonds are σ-and π- type between neighboring S atoms; 5-7 and 6-8. The superpositions of p_y, e.g. $\{(S)^5_{py} - (S)^7_{py}\}$, produces σ-bonds, whereas the π-bonds arise from p_x ao centered on neighboring S atoms, as $\{(S)^5_{px} + (S)^7_{px}\}$. The mo 95 and 96 are doubly degenerate E-symmetry, mo 96 being the highest occupied E symmetry mo. The character of both these mo is the S–As–S bonding. These are between all neighboring S atoms of each of the four As atoms and these are all π- bonds; there are four such combinations, 5-2-8, 5-3-7, 6-1-7, 6-4-8. The π-bonds consists of proper superpositions of s-, d-ao on the centered on arsenic and p-ao on the corresponding sulfur atoms; for example, the 5-2-8 π-bond $\{(S)^5_{py} + (As)^2_{dyy} + (S)^7_{py}\}$ as well as $\{(S)^5_{pz} + (As)^2_{dzz} + (S)^8_{pz}\}$. The mo 97 is the highest occupied mo of A_2 symmetry. It does not involve the As atoms at all, consisting of bonding between S atoms only. The bonding is solely π-type; between 5-7, and 6-8 involving p_y ao centered on corresponding S atoms and between 5-8 and 6-7 involving p_x ao, e.g. $\{S^5_{py} + S^7_{py}\}$ and $\{S^5_{px} + S^8_{px}\}$. In contrast molecular orbital 98, the highest occupied mo, has no electronic contributions from sulfur atoms at all, consisting of bonding between As atoms only. The bonding is between near neighbors 1-2 and 3-4 consisting of a set of σ- and π-bonds constructed from superposition of s-type and p_z-type ao, respectively, centered on the As atoms. To summarize the bonding in the α- As_4S_4 molecule, we have the dominant bonds being between the two pairs of near neighboring As atoms consisting of σ- and π- bonds from a superposition of s-, p- as well as the d- type ao. Showing the importance of including the d- ao basis on the As atoms. The next set are the neighboring As–S(e.g. 1-7, 1-6) bonds consisting of both the σ- and π- bonds from a superposition of s-, p- type ao the next important bond are between the S-atoms only consisting of again both σ- and π- bonds from a superposition of s-, p-type ao, and antibonding between neighboring pairs while slightly bonding between diagonal pairs. Thus, an arsenic atom is bonded directly with one other arsenic atom and each to two other sulfur atoms and in turn the four sulfur atoms are weekly bonded successively to the respective non-neighboring one.

2.2. Vibrational modes

Now we describe the vibrational modes of the α-As_4S_4 molecule. Further point group analysis for α-As_4S_4 with D_{2d} symmetry produces the following fundamental vibrational modes where the symmetry of each vibration is differentiated by the irreducible representation [20] that a given vibration transforms as:

$$\Gamma_{vib} = 3A_1(R) + 2A_2 + 2B_1(R) + 3B_2(R, IR) + 4E(R, IR)$$

That is, a total of 12 Raman bands and 7 IR bands. The high degree of symmetry of the molecule is helpful in making vibrational assignments. The assignments are determined using standard procedures whereby the traces of the symmetry operations are decomposed into the irreducible representations of the D_{2d} group.

For each of the vibrational modes assigned, one of three types of motion (As–As stretch, As–S stretch, As–S–As bend, and As–S–As wag) is visually assigned using the AVS Chemistryviewer [21] set of programs. The choice of internal coordinates is always somewhat arbitrary. However, we have found the above set to be complete and non-redundant. Other redundant coordinates, such as S–As–S motions, can be completely determined using the set of three motions given above. Our symmetry

analyses for the vibrational modes of As_4S_4 are presented in some detail to describe the basis for our assignments.

- As–As stretching modes: The two As–As single bonds form the basis of our analysis. The C_2 operator has a trace of two and the σ_d operator has a trace of two. All other operator except E have a trace of zero. Thus the symmetries are A_1 and B_2.
- As–S stretching modes: The eight As–S single bonds form the basis of our analysis. All operators expect E have a trace of zero. Thus the symmetries are A_1, A_2, B_1, B_2, and 2 E.
- As–S–As bending modes: The four As–S–As bending motions are the basis of our analysis. The C_2' operator has a trace of two. All other operators except E have a trace of zero. Thus the symmetries are A_1, B_1 and E.
- As–S–As wagging modes: The four As–S–As motions that are perpendicular to the As–S–As bond angle form the basis of our analysis. The C_2' operators has a trace of minus two. All other operators except E have a trace of zero. Thus, the symmetries are A_2, B_2, E.

By combining the results from the Chemistryviewer set of programs [21] with the symmetry considerations and our theoretical results for IR and Raman intensities, we are able to assign reported experimental IR and Raman results as shown in Tables 2–4. Raw frequencies for both the HF, B3LYP, and MP2 method are shown. Infrared intensities (km/mole) and Raman intensities (A^4/amu) are presented. B3LYP frequency calculations yield only the IR intensities as shown. The only allowed IR transitions are derived from vibrational modes having B_2 and E symmetries, and the only allowed Raman transitions are from vibrational modes having A_1, B_1, B_2 and E symmetries. The vibrational modes of symmetry A_2 are both IR and Raman forbidden.

3. Scaling vibrational frequencies

There are two types of molecular motions stretching and bending, once chemical bonds within the molecule have been established. The stretching vibration is a rhythmical movement along a bond axis. The bending vibration may consist of a change in bond angle; twisting, rocking and

Table 2
IR spectral analysis As_4S_4 (D_{2d}) performed at the HF at 6-311G* (frequency units in cm^{-1})

Symmetry	Normal mode	Calculated frequency	IR[a] intensity	Raman[b] intensity	Assignment	Experimental frequency[27]	Corrected frequency
A_1	ν_1	413	IR inactive	45	As–S stretch	355	361
	ν_2	254		21	As–S–As bend	196	209
	ν_3	214		14	As–As stretch	184	176
A_2	ν_4	378	Raman inactive	Raman inactive	As–S stretch	330	331
	ν_5	118			As–S–As wag	–	102
B_1	ν_6	397	IR inactive	15	As–S stretch	345	348
	ν_7	172		7	As–S–As bend	144	141
B_2	ν_8	421	41	3	As–S stretch	370	369
	ν_9	260	3	0	As–S–As wag	222	225
	ν_{10}	220	5	13	As–As stretch	173	181
E	ν_{11}	412	1	0	As–S stretch	376	360
	ν_{12}	398	31	6	As–S stretch	341	348
	ν_{13}	244	2	3	As–S–As bend	212	201
	ν_{14}	188	3	3	As–S–As wag	167	162

[a] Units of IR activity are km/mol.
[b] Units of Raman scattering activity are $Å^4$/amu.

Table 3
IR spectral analysis As_4S_4 (D_{2d}) performed at the DFT at 6-311G* (frequency units in cm^{-1})

Symmetry	Normal mode	Calculated frequency	IR[a] Intensity	Raman[b] Intensity	Assignment	Experimental frequency[27]	Corrected frequency
A_1	ν_1	362	IR Inactive	0	As–S stretch	355	368
	ν_2	219		11	As–S–As bend	196	206
	ν_3	177		16	As–As stretch	184	182
A_2	ν_4	305	IR Inactive	Raman Inactive	As–S stretch	330	309
	ν_5	107			As–S–As wag	–	104
B_1	ν_6	347	IR Inactive	0	As–S stretch	345	351
	ν_7	147		10	As–S–As bend	144	138
B_2	ν_8	364	22	0	As–S stretch	370	372
	ν_9	228	5	4	As–S–As wag	222	225
	ν_{10}	171	1	7	As–As stretch	173	175
E	ν_{11}	366	1	0	As–S stretch	376	373
	ν_{12}	335	27	2	As–S stretch	341	340
	ν_{13}	218	2	3	As–S–As bend	212	205
	ν_{14}	165	2	3	As–S–As wag	167	163

[a] Units of IR activity are km/mol.
[b] Units of Raman scattering activity are $Å^4$/amu.

wagging are each specialized forms of a bending vibration.

Interpretation of an experimental IR spectrum of a complex molecule is complex. It is often built up by some 'rule of thumb 'empirical facts. There exists a vast compilation of such data for organic molecules [22]. For example, the CO stretching frequencies in alcohols and phenols produce a strong band in the 1260–1000 cm^{-1} region, while aliphatic aldehydes absorb near 1740–1720 cm^{-1}. The carboxylate group, $[O–C–O]^-$, has two strongly coupled C–O bond stretches giving a strong asymmetrical stretching band near 1600 cm^{-1} and a weaker symmetrical stretching band near 1400 cm^{-1}. Lack of strong absorption in the 909–650 cm^{-1} region generally

Table 4
IR spectral analysis As_4S_4 (D_{2d}) performed at the MP2 at 6-311G* (frequency units in cm^{-1})

Symmetry	Normal mode	Calculated frequency	IR[a]Intensity	Assignment	Experimental frequency[27]	Corrected frequency
A_1	ν_1	383	IR Inactive	As–S stretch	355	366
	ν_2	227		As–S–As bend	196	206
	ν_3	188		As–As stretch	184	182
A_2	ν_4	332	IR Inactive	As–S stretch	330	317
	ν_5	109		As–S–As wag	–	103
B_1	ν_6	371	IR Inactive	As–S stretch	345	355
	ν_7	153		As–S–As bend	144	139
B_2	ν_8	381	18	As–S stretch	370	364
	ν_9	237	5	As–S–As wag	222	225
	ν_{10}	182	1	As–As stretch	173	175
E	ν_{11}	389	1	As–S stretch	376	372
	ν_{12}	356	24	As–S stretch	341	340
	ν_{13}	225	2	As–S–As bend	212	205
	ν_{14}	172	1	As–S–As wag	167	163

[a] Units of IR activity are km/mol.

indicates a non-aromatic structure. The absence of absorption in the assigned ranges for the various functional groups can usually be used as evidence for the absence of such a group in the molecule.

A similar compilation of data and empirical rules for inorganic molecules would be very helpful. We have been calculating vibrational frequencies for some types of inorganic molecules for the last ten years at different levels of the theory and comparing the results with the experimental data. Most recently studies involving P_4S_{10} [23], P_4S_3/P_4S_7 [24], and P_4O_6 [25] were reported. This manuscript is another of the series in which we shall also undertake scaling of the computed frequencies and classify different vibrations of an inorganic molecule in terms of stretching and bending of bonds between P and O atoms in different configurations and come up with a sound scaling procedure. The aim is to perform, using the same procedure, a fair number of inorganic molecules with the hope that some trend shall emerge and be helpful to make connection between computed and observed frequencies.

Computations of vibrational frequencies at different levels of accuracy, from HF/3-21G to MP2/6-31G* for small to moderate size molecules, H_2 to perylene ($C_{20}H_{12}$), show that the computed frequencies are generally 5–10% higher than the corresponding experimental values. Observations of empirical data shows that similar localized motions, e.g. all P–O stretches of a molecule will have a similar scaling factor (computed frequency: experimental frequency ratio). Similarly, all vibrations identifiable as P–O–P bends will have another near constant scaling factor. It is also our bias that such scaling procedures have to be essentially empirical; there are just too many complicated variables (e.g. choice of basis, Hamiltonian, and the molecular system, let alone the experimental variables) to make a reasonable causal connection. We have thus resorted to an empirical scheme, which would be simple to consistently apply without requiring too much physical intuition. Having tried out several such schemes. Let $\{\nu_{\text{expt,i}}\}$ and $\{\nu_{\text{calc,i}}\}$, respectively, correspond to the experimental and computed frequencies for the same group of vibrations, e.g. all in the P–O stretch group:

1. (i) averaging the ratio between the experimental and computed frequencies;
2. (ii) Minimizing the mean square error, $Q = \sum_i (\lambda\nu_{\text{calc,i}} - \nu_{\text{expt,i}})^2$; and
3. (iii) Minimizing the weighted mean square error, $R = \sum_i W_i(\lambda\nu_{\text{calc,i}} - \nu_{\text{expt,i}})^2$, where the weight w_i is transition probability chosen to have the experimental or the computational value. Whenever such weights are available this procedure yields better fit for the vibrational frequencies.

However, based upon the criteria of simplicity, uniformity and reasonable accuracy the mean square error Q is our final choice. The condition for the computed frequencies scaled by a factor λ, be such that the mean square error, $Q = \sum_i (\lambda\nu_{\text{calc,i}} - \nu_{\text{expt,i}})^2$ be a minimum is, the stationary condition $dQ/d\lambda = 0$. This determines the $\lambda = \sum_i \times \nu_{\text{calc,i}}\nu_{\text{expt,i}}/\sum_i (\nu_{\text{calc,i}})^2$. Furthermore, $d^2Q/d\lambda^2 = 2\sum_i (\nu_{\text{calc,i}})^2 > 0$, shows that this value of λ corresponds to a minimum in Q.

Based on use of the procedure proposed in Section 2, a set of correction factors used for the different types of vibrational modes. These correction factors are determined by taking the average of the ratios between the computed and experimental frequencies for a particular mode, e.g. a As–S stretch. From these correction factors, the corrected frequencies are derived and presented in Tables 2–4. In these tables the quality of fitting is indicated by the root-mean-square standard deviation, $\sigma = \{\sum_i (\nu_{\text{pred,i}} - \nu_{\text{expt,i}})^2/N\}^{1/2}$ where N is the number of unique normal modes (14 for As_4S_4), which yields the following values:

HF (26 cm^{-1}), MP2 (15 cm^{-1}) and DFT/B3LYP (11 cm^{-1})

The small variation observed in these correction factors indicates that the procedure should provide reliable predictions. A vector diagram [26] for each of the 24 corrected normal modes of vibration for As_4S_4 is presented in Fig. 3.

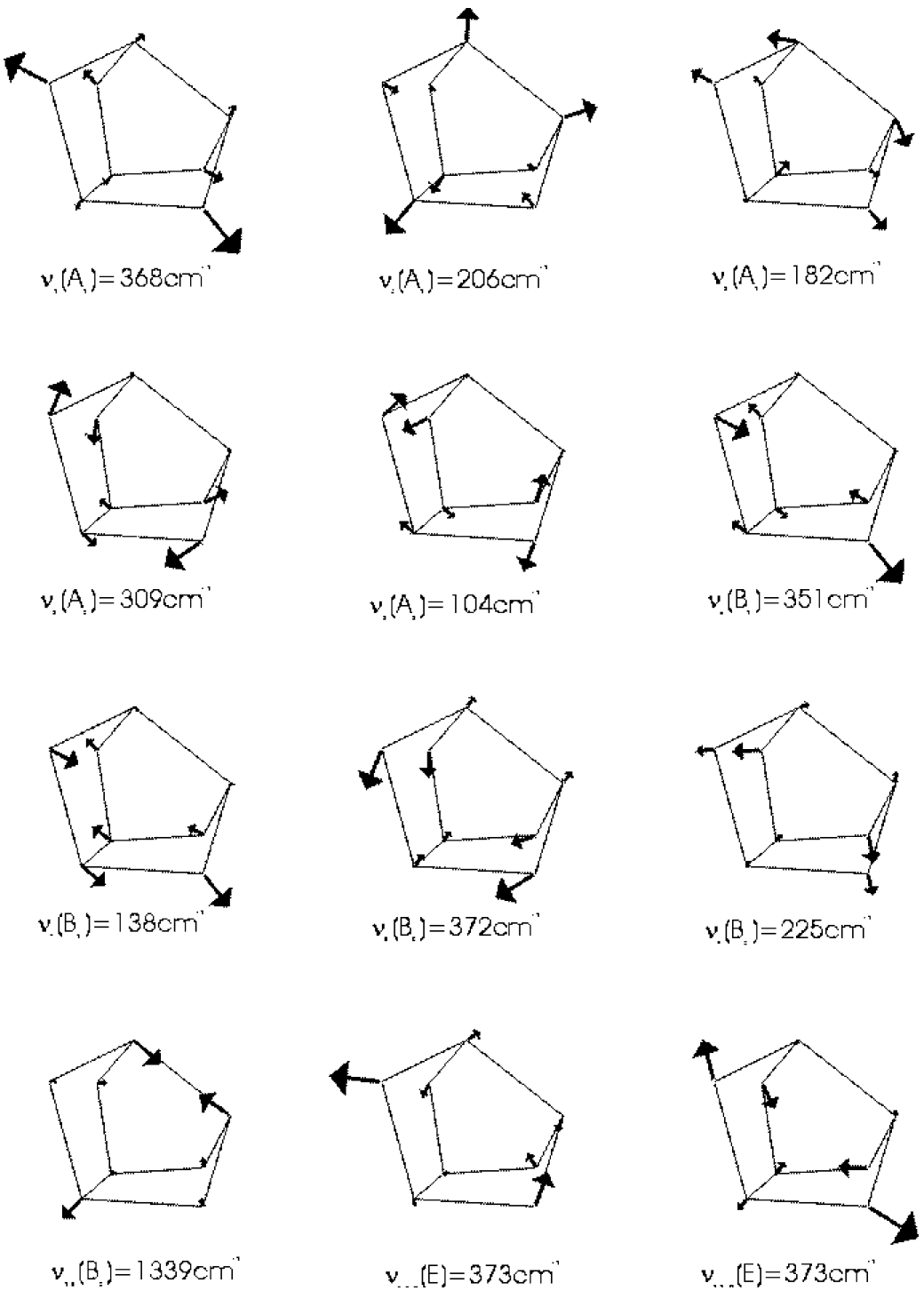

Fig. 3. Normal modes of As_4S_4.

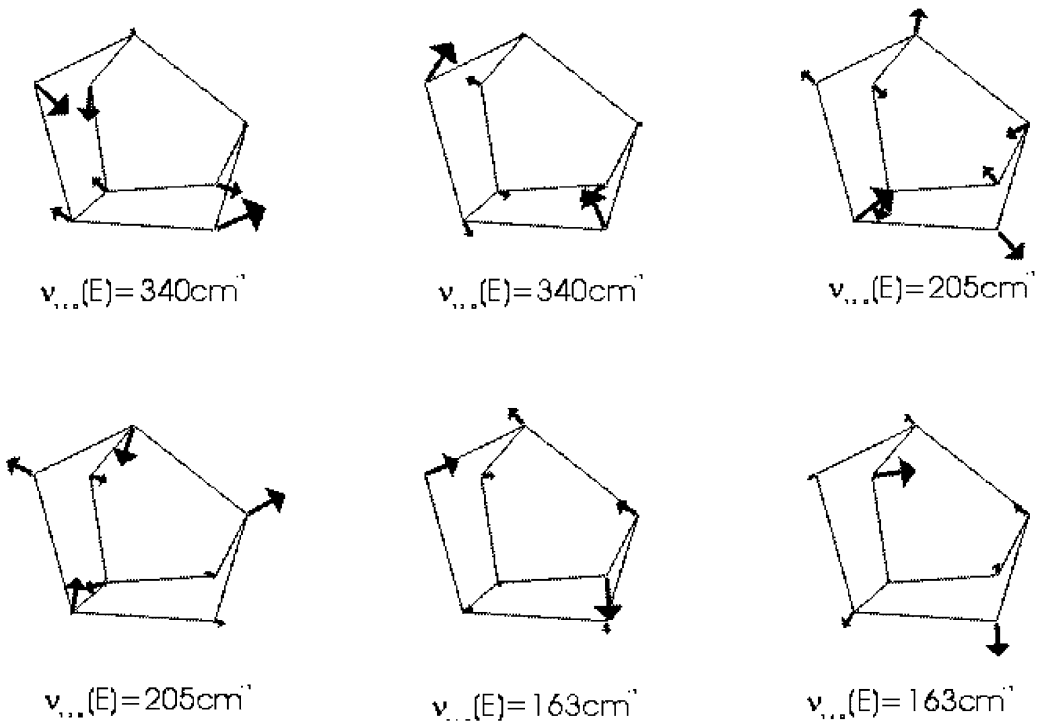

Fig. 3 (*continued*)

Acknowledgements

We express our appreciation to The U.S. Army Edgewood Research, Development and Engineering Center, U.S. Army, for support of this work as part of the Standoff Detection Project, Project Number 1C162622A553C, Reconnaissance, Detection and Identification.

References

[1] G.C. Chern, I. Lauks, J. Appl. Phys. 53 (1982) 6979.
[2] N. Tohge, S.C. Moss, S.R. Ovshinski, J. Non-crystallogr. Solids 13 (1973) 191.
[3] A. Kutoglu, Z. Anorg. Chem. 419 (1976) 176.
[4] A.C. Roberts, H.G. Ansell, M. Bonardi, Can. Mineral 18 (1995) 525.
[5] P. Bonazzi, S. Menechetti, Pratesi, Am. Mineral 80 (1995) 400.
[6] D.L. Douglass, C. Shing, G. Wang, Am. Mineral 77 (1992) 1266.
[7] D.J.E. Mullen, W. Nowacki, Z. Kristallogr. 136 (1972) 48.
[8] E.J. Porter, G.M. Sheldrick, J. Chem. Soc. Dalton Trans. 13 (1972) 1347.
[9] D. Babić, S. Rabii, Phys. Rev. B 39 (1989) 10831.
[10] D. Babić, S. Rabii, Phys. Rev. B 38 (1988) 10490.
[11] T. Yamabe, K. Tanaka, A. Tachibana, Y. Kobayashi, H. Teramae, K. Fukui, Solid State Commun. 40 (1981) 521.
[12] H.J. Whitfeld, J. Chem. Soc. Dalton trans. 12 (1973) 1740.
[13] P. Goldstein, P. Paton, Acta Crystallogr. Sect. B 30 (1974) 915.
[14] W.J. Hehre, L. Radom, P.V.R. Schleyer, J.A. Pople, Ab Initio Molecular Orbital Theory, Wiley, New York, 1986.
[15] C. Mø, M.S. Plesset, Phys. Rev. 46 (1934) 618–622.
[16] R.G. Parr, W. Yang, Density-Functional Theory of Atoms and Molecules, Oxford, New York, 1989.
[17] A.D. Becke, J. Chem. Phys. 98 (1993) 5648–5652.
[18] C. Lee, W. Yang, R.G. Parr, Phys. Rev. B 37 (1988) 785–789.
[19] M.J. Frisch, G.W. Trucks, H.B. Schlegel, G.E. Scuseria, M.A. Robb, J.R. Cheeseman, V.G. Zakrzewski, J.A. Montgomery, Jr., R.E. Stratmann, J.C. Burant, S. Dapprich, J.M. Millam, A.D. Daniels, K.N. Kudin, M.C. Strain, O. Farkas, J. Tomasi, V. Barone, M. Cossi, R. Cammi, B. Mennucci, C. Pomelli, C. Adamo, S. Clifford, J. Ochterski, G.A. Petersson, P.Y. Ayala, Q. Cui, K. Morokuma, N. Rega, P. Salvador, J.J. Dannenberg, D.K. Malick, A.D. Rabuck, K. Raghavachari, J.B. Foresman, J. Cioslowski, J.V. Ortiz, A.G. Baboul, G. Stefanov Liu, A. Liashenko, P. Piskorz, I. Komaromi, R. Gomperts, R.L. Martin, D.J. Fox, T. Keith, M.A. Al-Laham, C.Y. Peng, A. Nanayakkara, M. Challacombe, P.M.W. Gill, B. Johnson, W. Chen, M.W. Wong, J.L. Andres, C. Gonzalez, M.

Head-Gordon, E.S. Replogle, J.A. Pople, GAUSSIAN 98, Revision A.11.2, Gaussian Inc., Pittsburgh PA, 2001.
[20] F.A. Cotton, Chemical Applications of Group Theory, Wiley Interscience, New York, 1971.
[21] A.B. Nielsen, A.J. Holder, Gauss View User's Reference, Version 2.0, Gaussian Inc.,Pittsburgh PA, 1998.
[22] R.M. Silverstein, G.C. Bassler, T.C. Morrill, Spectrometric Identification of Organic Compounds, Fifth ed., Wiley, New York, 1991.
[23] J.O. Jensen, D. Zeroka, A. Banerjee, J. Mol. Struct. (Theochem.) 505 (2000) 31–43.
[24] J.O. Jensen, D. Zeroka, J. Mol. Struct. (Theochem.) 487 (1999) 267–274.
[25] J.O. Jensen, A. Banerjee, C.N. Merrow, D. Zeroka, J.M. Lochner, J. Mol. Struct. (Theochem.) 531 (2000) 323–331.
[26] Mukherjee, A., Spiro, T.G. The Svib Program: An Expert System for Vibrational Analysis, QCPE Program 656, Indiana University, 1995.
[27] M. Muniz-Miranda, G. Sbrana, P. Bonazzi, S. Menchetti, G. Pratesi, Spectrochim. Acta Part A 52 (1996) 1391.
[28] A.C. Chapman, Spectrochim. Acta 24A (1968) 1687–1696.